

Light Band Zone Formation and its Influence on Properties of Magnetically Impelled Arc Butt (MIAB) Welded Carbon Steel Tubes

R. Sivasankari¹ · V. Balusamy¹ · P. R. Venkateswaran² · K. Ganesh Kumar² · G. Buvanashakaran²

Received: 17 March 2017 / Accepted: 25 July 2017 / Published online: 9 August 2017
© The Indian Institute of Metals - IIM 2017

Abstract Magnetically Impelled Arc Butt (MIAB) welding is a solid state welding process especially used in circumferential butt welding of tubes in which heat is generated prior to upsetting by an electric arc moving along the peripheral edges of the weldment with the aid of an external magnetic field. This paper aims at studying the formation of Light Band (LB) zone and its effect on the weld properties of MIAB welding of carbon steel tubes. A detailed microstructural analysis has been carried out to understand the microstructural transformations taking place in Thermo-Mechanically Affected Zone leading to formation of LB zone. Welded samples show better tensile properties with higher upset current as it eliminates LB zone formation at weld interface. For lower upset current, width of the LB zone increases with increase in arc rotation current resulting in lower weld tensile strength.

Keywords MIAB · Welding · TMAZ · Decarburized · Light-band · Acicular

1 Introduction

Magnetically Impelled Arc Butt (MIAB) welding utilizes the principle of forge welding for joining of materials in solid state. Heating of the faying surfaces is carried out through an electric arc and after sufficient heating, an upsetting force is applied. A static, radial magnetic field is used to cause the arc to rotate along the circumference of

the tubes. Rotation of the arc takes place due to interactive effect of the external magnetic field on the arc current. During arc rotation, speed of the arc is quite high (150 m/s or greater). Arc rotation causes uniform heating of faying surfaces. Finally, upsetting is done after sufficient melting of faying surface producing a solid state bond with a characteristic flash [1].

In the work conducted by Akira Taneko et al., the velocity of the rotating arc was studied with the aid of a high speed camera. The velocity of the rotating arc was considered to lie in the low velocity region or high velocity region or speed fluctuation region, depending on certain defined characteristics related to heating of the pipes. Condition for obtaining a good bonding was postulated in this work [2].

The external magnetic field was found to have considerable influence on the rotating arc and the weld properties [3]. Numerical models were suggested to relate the external magnetic fields with MIAB parameters like welding current and exciting current [4].

D. Iordachescu et al. studied six different process stages in MIAB welding starting from the arc initiation to joint formation, namely arc initiation, arc rotation starting, transitory arc, arc rotation, arc termination and the application of upsetting force. They also presented the essential variables influencing the weld defect formation [5]. Arungalai Vendan et al. [6] reported feasibility of using MIAB process for joining high thick components. Effect of structural changes on weld properties in MIAB welded T11 steel tubes was reported by Sivasankari et al. [7]. MIAB welding parameters were found to play significant role in producing defect free joints.

Formation of microstructural features due to faster heating and cooling plays a significant effect on the joint characteristics in any welding process. The characteristic

✉ R. Sivasankari
rshivasankari@gmail.com

¹ PSG College of Technology, Coimbatore, India

² Welding Research Institute, BHEL, Tiruchirappalli, India

thermal history produced by MIAB welding results in the formation of Light Band (LB) zone at the weld interface. In this work, an attempt has been made to study the effect of LB zone on mechanical properties of MIAB weldments. Detailed effects of MIAB welding parameters on weld properties have not been much reported in the earlier works. Present work attempts to make a detailed study on microstructural transformations and mechanical properties of MIAB welded carbon steel tubes.

2 Experimental Work

2.1 Material

Carbon steel tubes with outer diameter of 44 mm and thickness of 4.5 mm were used for welding. The chemical composition (wt%) of the steel is 0.27 C, 0.156 Si, 0.530 Mn, 0.0084 P and 0.011 S. The carbon steel has average yield strength of 258 MPa, average tensile strength of 442 MPa and average hardness of 147 HV @ 100 g load.

2.2 MIAB Welding of Medium Carbon Steel Tubes

Welding trials were conducted in Welding Research Institute (WRI) of BHEL, Tiruchirappalli, India using a hydraulic MIAB welding machine.

MIAB welding process is divided into four stages namely arc initiation, arc stabilization, arc rotation and upsetting based on the welding time period. Arc initiation is caused by a sequence of three step operation including shorting the gap between the tubes, retracting the tubes through a fixed gap and then striking the arc between the tubes. In the next stage of arc stabilization, arc starts to rotate slowly along the inner diameter of the tube ends. During arc rotation, arc accelerates and rotates with high speed along the outer diameter of the tubes thus heating up the faying surfaces to red hot condition. After sufficient melting, upsetting action takes place resulting in flashing of the molten metal and solid state joining of the tubes.

To establish parametric window for the welding variables, initial welding trials were conducted on trial and error basis. The parameters that resulted in full penetration and adequate flash formation were chosen for DoE analysis. Table 1 shows the actual welding trials designed using factorial method. DoE trials were created by half factorial method using Minitab 16 software. For all the welding trials, tube gap and upset pressure were fixed as 2 mm and 16 MPa respectively.

2.3 Characterization of MIAB Welded Samples

Microstructural analysis involved the characterization of microstructural variation in Thermo-Mechanically

Table 1 MIAB welding trials

Sample identification	I ₁ (A)	I ₂ (A)	I ₃ (A)	T ₂ (s)	T ₃ (s)
CS/1	330	310	1000	6	12
CS/2	300	280	600	6	8
CS/3	330	280	1000	4	12
CS/4	330	310	1000	4	8
CS/5	330	280	600	6	12
CS/6	300	310	600	4	8
CS/7	300	310	1000	6	8
CS/8	330	280	1000	6	8
CS/9	300	310	600	6	12
CS/10	300	310	1000	4	12
CS/11	300	280	1000	6	12
CS/12	330	310	600	6	8
CS/13	330	280	600	4	8
CS/14	300	280	600	4	12
CS/15	300	280	1000	4	8
CS/16	330	310	600	4	12

Affected Zones (TMAZs) of the welded tubes by optical and electron microscopy. Mechanical tests included hardness test, tension test and bend test. From the results, the structure property correlation was evolved. Using DoE analysis, individual effect and interaction effect of the welding parameters on weld properties were studied.

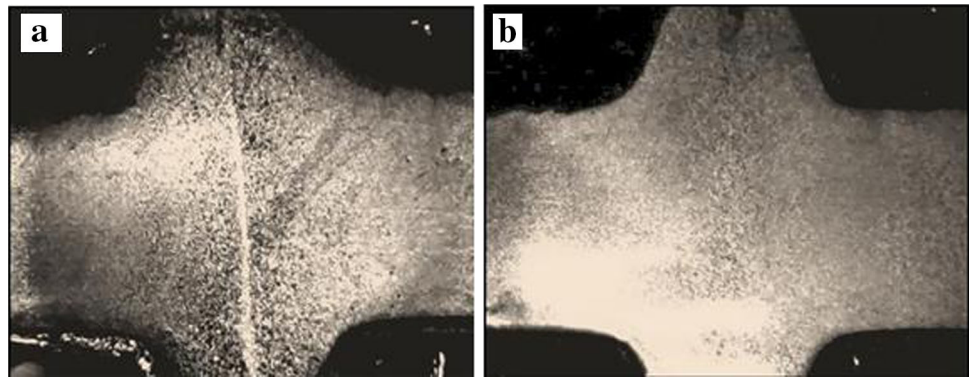
For microstructural analysis, the joints were sectioned transverse to welding direction and the sectioned specimen were polished and etched with 2% Nital solution. Transverse tension test and bend test of the MIAB welded samples were carried out in accordance with ASTM A370 standard.

3 Results and Discussion

3.1 Macrostructural Analysis

An important feature revealed from the macroexamination is the presence of a distinct white zone along the weld interface (Fig. 1). This white zone was referred as Light Band (LB) zone in the earlier works of Zak and Rys [8] and Oshkaderov [9]. LB zone at the weld interface is the decarburized zone formed due to chemical inhomogeneity. Chemical inhomogeneity causing decarburization in LB zone occurs due to incomplete homogenization and upsetting. Initially, the microstructure of the carbon steel tubes contains ferrite and pearlite phases at room temperature. During welding, when heated to above the critical temperature, solid state phase transformation occurs. Lamellar pearlite containing alternate ferrite and cementite forms metastable eutectic mixture at the interface of two

Fig. 1 Macrostructures of MIAB welded carbon steel tubes at 15 X



phases. However the ferrite phase transforms to austenite above critical temperature. At a temperature of about ~ 1150 °C, the eutectic mixture melts ahead of austenite resulting in formation of high carbon liquid metal and low carbon solid austenite. Complete homogenization does not happen as the rate of heating is high. Upon upsetting, the high carbon liquid metal is expelled as flash. The retained low carbon austenite is transformed into LB zone with more ferritic structure [9].

The LB zone formation is more predominant in samples welded with lower upset current (Fig. 1a). Upset current is the short pulse of high current given prior to the upsetting to expel the molten metal and impurities into flash. Hence the lower upset current (600 A) chosen for MIAB welding is not sufficient to remove the LB zone from the weld interface. As the upset current increases, the LB zone formation decreases since the decarburized zone is expelled along with the molten metal as flash at higher current levels (Fig. 1b).

3.2 Microstructural Analysis

Depending on thermal gradient and deformation due to upsetting, in each of the weldments, three distinct TMAZs have been formed from weld interface to unaffected base metal. Figure 2 shows the microstructure of TMAZs present in sample CS/1. TMAZ I is the zone present at the weld interface. TMAZ I shows multiphase microstructure of acicular ferrite, pearlite and grain boundary ferrite with a few Widmanstatten ferrite (Fig. 3a, b). Acicular ferrite (about 46%) and pearlite (about 35%) have been found to be predominant.

Austenite deformation leads to refinement in its grain size and thereby increases the nucleating site for ferrite and pearlite at austenite grain boundaries. Presence of acicular ferrite is the most desirable weld structure as it improves weld toughness [10, 11]. Acicular ferrite contains intragranular ferrite sheaves due to faster cooling [12, 13]. Figure 3a shows the acicular ferrite laths in TMAZ I. Deformation caused during upsetting significantly

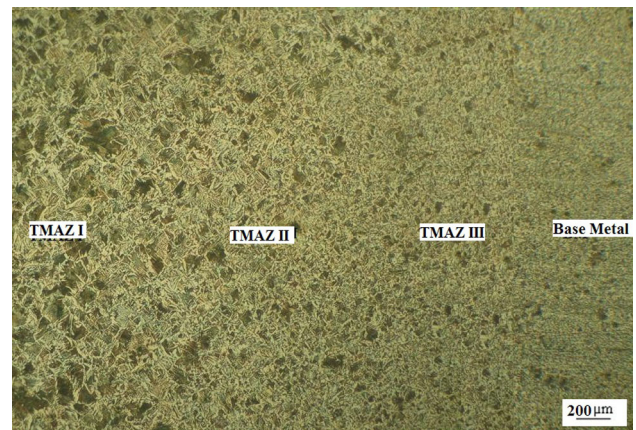


Fig. 2 Microstructure of Sample CS/1

influences the formation of acicular ferrite. Plastic deformation of austenite causes increase in dislocation density. The dislocation can act as the nucleation site for acicular ferrite. The faster cooling serves as chemical driving force in acicular ferrite nucleation. Apart from nucleation, plastic deformation also influences the growth of acicular ferrite. As the defect density increases, it retards the growth of ferrite laths in acicular ferrite. Since the defects hinder the growth of ferrite laths, it results in shorter acicular ferrite formation [14, 15]. With faster cooling, the formation of bainite is retarded due to presence of grain boundary ferrite. As austenite grain boundaries are the nucleating sites for bainite transformation, presence of grain boundary ferrite prevents the nucleation of bainite [16].

With decreased cooling rate, the microstructure of TMAZ II shows predominantly polygonal ferrite and pearlite (Fig. 4a, b). In TMAZ III, the microstructure shows normalized structure with fine grains of ferrite and pearlite (Fig. 5a, b). TMAZs of all the welded samples show similar microstructure in TMAZ II and TMAZ III. Figure 6a, b shows the microstructure of unaffected base metal with fine ferrite and pearlite.

In TMAZ I, the microstructure varies with welding parameters. The LB zone formation is apparent in the

Fig. 3 Microstructure of TMAZ I in sample CS/1

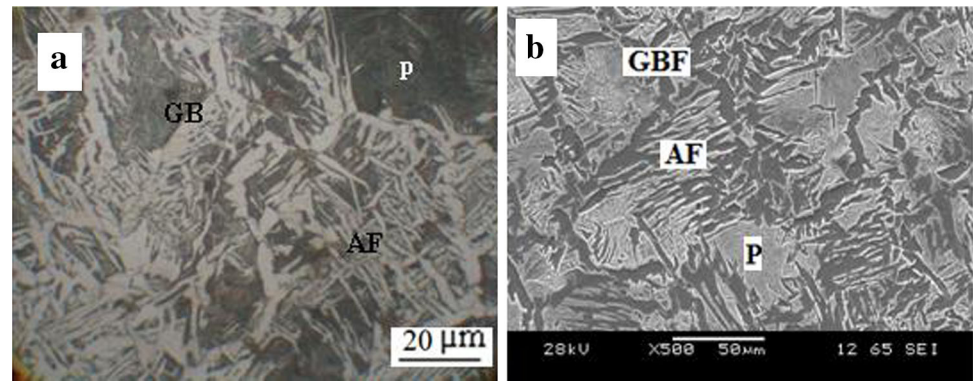
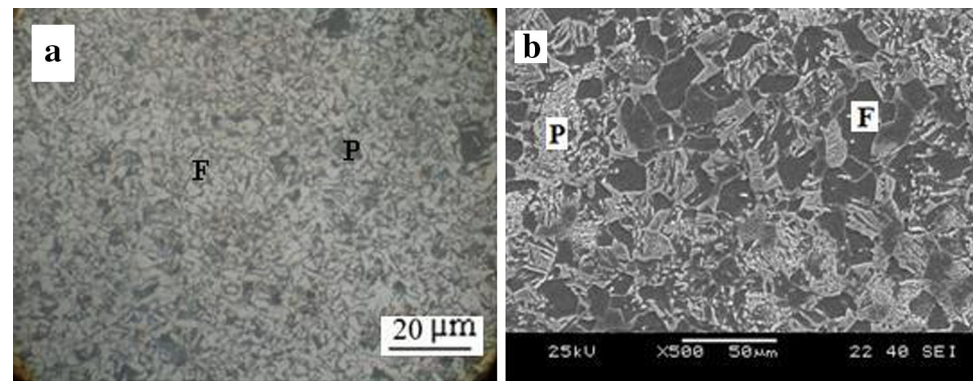


Fig. 4 Microstructure of TMAZ II in sample CS/1



samples welded with lower upset current. The microstructure of sample CS/9 welded with lower upset current is shown in the Fig. 7. The microstructure along the weld interface shows LB zone with predominantly polygonal ferrite (about 78%) along with acicular ferrite (about 11%). Some Widmanstatten ferrite side plates (Fig. 7a, b), extending from polygonal grains, have also been observed locally [17, 18]. Due to incomplete homogenization and insufficient expulsion, weld interface become depleted of carbon causing more ferrite structure at the interface. LB zone contains mixture of ferrite morphology with predominantly polygonal ferrite. Decarburized zone at the weld interface is heated up to higher temperature compared to adjacent region. Higher deformation temperature of

austenite with lower upset current results in lower defect density at the weld interface [19]. The volume fraction of acicular ferrite decreases as nucleation site decreases. Adjacent to LB zone, TMAZ I shows a multiple phase microstructure containing acicular ferrite, pearlite and grain boundary ferrite.

3.2.1 Effect of Upset Current

The lower upset current (600 A) used is not sufficient for complete expulsion of the decarburized zone and hence it has resulted in formation of LB zone with more ferritic structure along the welded interface. With higher upset current (1000 A), the decarburized zone gets expelled as

Fig. 5 Microstructure of TMAZ III in sample CS/1

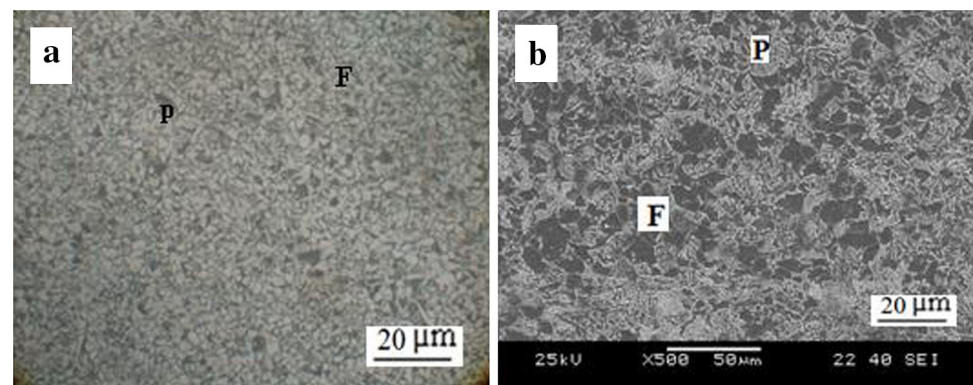
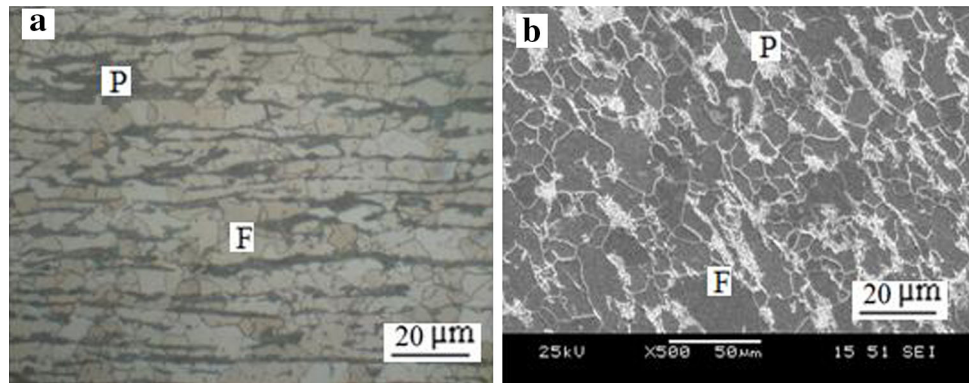
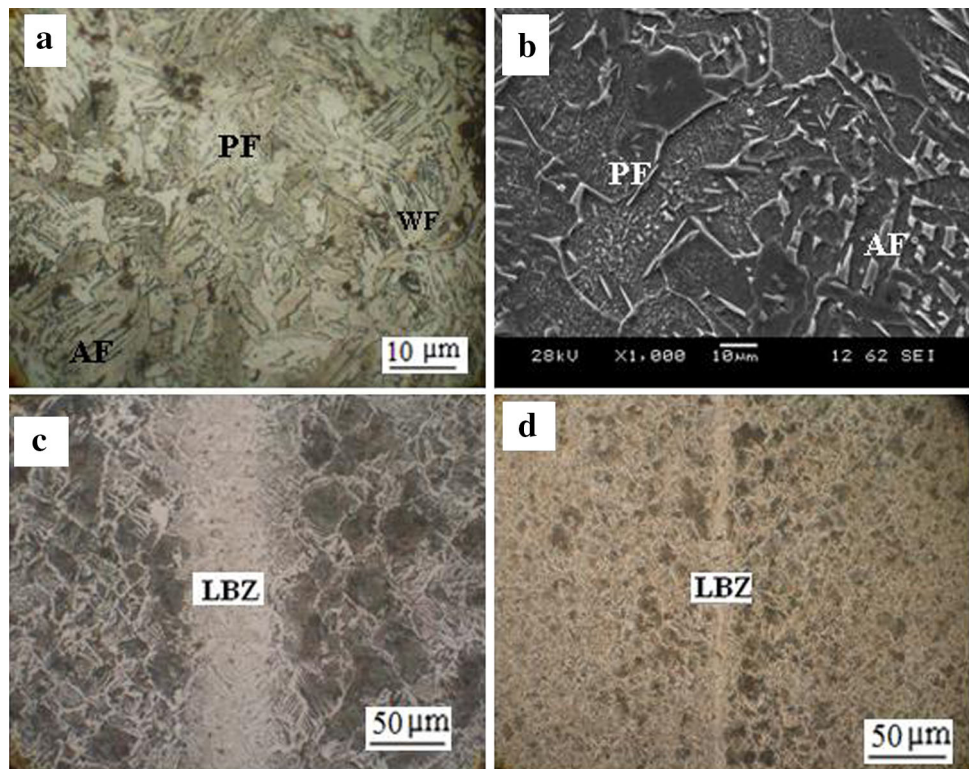


Fig. 6 Microstructure of unaffected zone**Fig. 7** Microstructure of weld interface in samples welded using lower upset current. (a, b) Sample CS/9, (c) sample CS/12 and (d) sample CS/14

flash resulting in multiphase microstructure containing acicular ferrite, pearlite and grain boundary ferrite.

3.2.2 Effect of Arc Rotation Current

The effect of arc rotation current is more prominent with lower upset current. Irrespective of any value for the arc rotation current, the samples welded with higher upset current show similar microstructures. With lower upset current, the width of LB zone along the weld interface seems to increase with increase in arc rotation current (Fig. 7c, d). Higher arc rotation current causes more melting with larger plasticized material resulting in wider LB zone at the weld interface. The volume fraction of acicular ferrite is lower in the samples welded at higher arc

rotation current and lower upset current. Decrease in volume fraction is due to retained high temperature zone at weld interface. Higher deformation temperature results in lower internal stored energy and results in reduced efficacy of dislocation in promoting acicular ferrite [20].

3.2.3 Effect of Arc Rotation Time

The arc rotation time has less significant effect on LB zone formation at the weld interface. When arc rotation time increases, melting also increases causing more plasticized metal next to molten metal which in turn can be expelled easily from the interface. Hence in case of samples welded with lower arc rotation current and lower upset current, the width of LB zone decreases marginally with increase in arc

rotation time. With higher arc rotation current, the width of LB zone increases marginally with increase in arc rotation time as it leads to excess melting within large plasticized zone at the faying surfaces.

3.3 Transverse Tension Test

Transverse tension testing has been carried out to assess the weld strength of MIAB welded samples. As transverse tension specimen contains all the TMAZs and the unaffected parent metal, the failure is expected to occur at the weaker region. In tension testing, the maximum load and region of failure have been noted for each sample. In case of stronger weld, failure occurs at the base metal. Tension test results are tabulated in Table 2. Presence of LB zone weakens the weld tensile strength. This is due to decarburization causing more ferritic structure at weld interface. Thus during tension test, the LB zone having inferior strength fails. Though all the samples welded with lower upset current contains LB zone at weld interface, a few samples show failure at base metal also. Failure at the weld interface is predominant in the samples welded with higher arc rotation current and lower upset current. This is because the width of LB zone is high at higher arc rotation current. With lower upset current, the width of LB zone is about 325–482 μm for sample welded with higher arc rotation current in contrast to samples welded with lower arc rotation current having LB zone width of about 20–55 μm . Failure is less frequent in the samples with narrow LB zone at the weld interface.

With narrow LB zone at the weld interface, the microstructure contains less volume fraction of polygonal

ferrite compared to the samples welded with higher arc rotation current. Hence the weld is less likely to fail with lower arc rotation current and lower upset current. UTS of the samples show lower tensile strength for samples (CS/6, CS/9, CS/12, CS/16) welded with higher arc rotation current and lower upset current compared to samples (CS/2 and CS/13) welded with lower arc rotation current and lower upset current. Also the UTS values of samples welded with lower arc rotation current are close to the UTS of the base metal.

3.3.1 SEM Analysis of Tension Test Specimen

SEM micrographs of the tensile fracture surface of tension test specimens are shown in Fig. 8. The fracture surface of samples failed at the base metal show cup and cone fracture (Fig. 8a) containing dimples with microvoids (Fig. 8c). All the samples failing at the unaffected base metal show similar ductile type of fracture. Fracture surface of the samples failing at the weld interface shows flat and granular surface with reduced elongation compared to samples failing at base metal (Fig. 8b). SEM micrographs of samples failing at weld interface show intergranular brittle fracture (Fig. 8d). Though the LB zone contains softer and tougher microstructure, the induced brittleness is due to the presence of impurities at the weld interface. Apart from LB zone formation, lower upset current also causes retention of oxide impurities at the weld interface. EDX analysis (Fig. 9) at tension test fracture surface in sample CS/12 shows that the impurities are mostly oxides containing mainly Si, Fe and Al with minor Mn and S. The presence of oxides and their high density indicate the retention of impurities due to incomplete expulsion. These oxides will affect the ductility of weld as they act as stress raiser and potential site for crack formation.

3.3.2 DoE Analysis of Tension Test Results

Figure 10 shows the individual parameter effect on UTS of the welded tubes. In correlation with microstructural analysis, the upset current and arc rotation current show significant individual parameter effect as they control the formation of LB zone at the weld interface. Lower arc rotation current and higher upset current show positive effect on UTS as they cause narrow LB zone at the weld interface.

The significance of the welding variables has been calculated using regression analysis. The relation between the weld UTS and the welding variables is given in Eq. (1). This model in terms of coded variables, report R^2 of 87.17%, adjusted R^2 of 79.5% and a root-mean-square error 'S' of 22.9 MPa. The relative significance of the welding variable is shown in the half normal plot (Fig. 11).

Table 2 Tension test results of MIAB welded carbon steel tubes

Sample identification	UTS (MPa)	Region of failure
CS/1	443 \pm 21.2	Base metal
CS/2	432 \pm 21.6	Weld interface
CS/3	445 \pm 22.3	Base metal
CS/4	471 \pm 23.6	Base metal
CS/5	459 \pm 23	Base metal
CS/6	373 \pm 18.7	Weld interface
CS/7	463 \pm 23.1	Base metal
CS/8	459 \pm 25	Base metal
CS/9	286 \pm 14.3	Weld interface
CS/10	460 \pm 21.5	Base metal
CS/11	471 \pm 23.6	Base metal
CS/12	397 \pm 19.9	Weld interface
CS/13	426 \pm 21.3	Weld interface
CS/14	447 \pm 22.4	Base metal
CS/15	455 \pm 22.8	Base metal
CS/16	358 \pm 17.9	Weld interface

Fig. 8 Tension test specimens after testing, SEM micrographs of fractured tension test specimens. (c Sample CS/1, d sample CS/13)

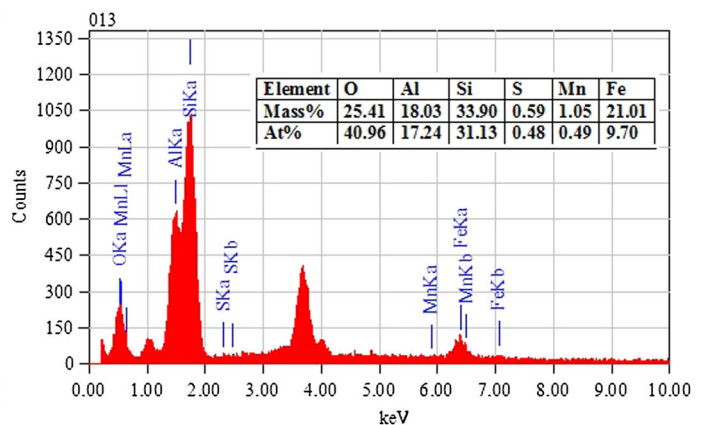
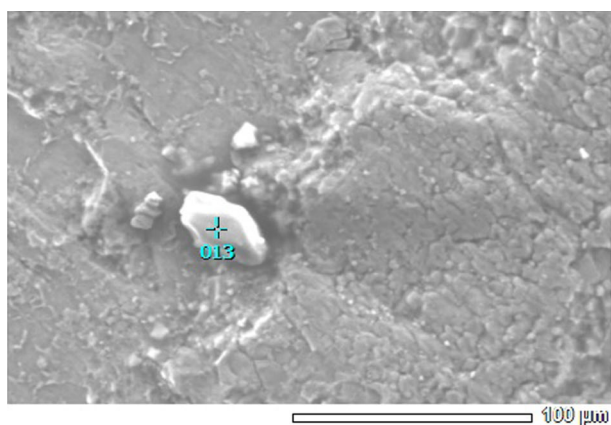
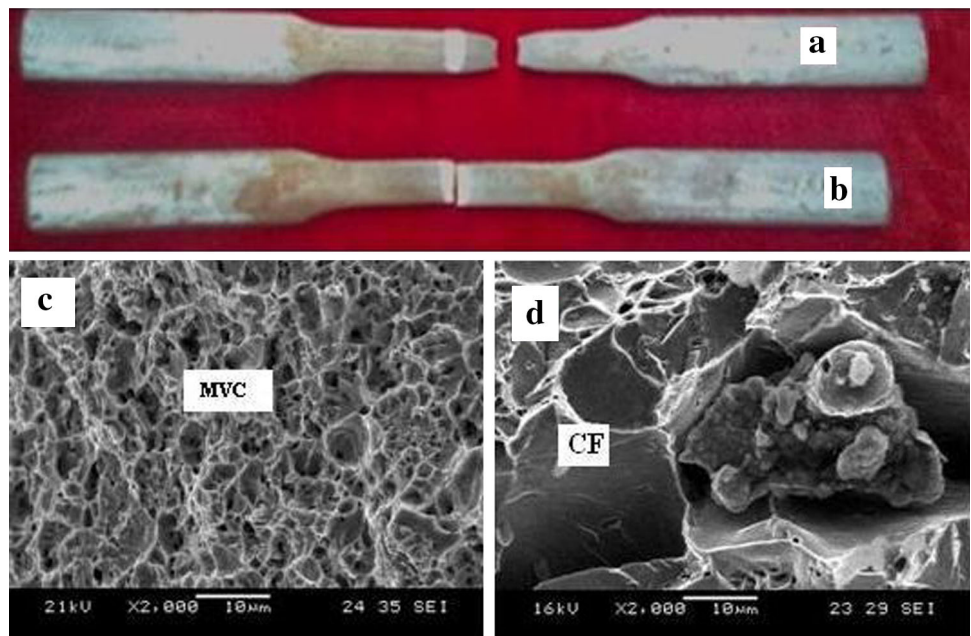


Fig. 9 EDX analysis of tensile fractured surface in sample CS/12

The variables lying away from the straight line are considered relatively dominant at a level of significance of $\alpha = 0.05$.

$$\begin{aligned}
 \text{UTS(MPa)} = & 427.81 - 21.44 \times B + 30.56 \times C - 6.69 \\
 & \times E + 22.31 B \times C - 12.94 B \times E \\
 & + 3.06 C \times E
 \end{aligned}
 \tag{1}$$

Interaction effect plot for MIAB welding parameters is shown in Fig. 12. Interaction effects of the welding parameters are analyzed using UTS as the response variable. Upset current shows the most significant effect on the tensile strength as it controls the formation of LB zone at the weld interface. Upset current and arc rotation current show significant interactive effect on weld tensile strength. At higher upset current, arc rotation current does not influence

the weld tensile strength as complete expulsion of LB zone takes place at the weld interface. At lower upset current, the width of LB zone is influenced by arc rotation current. Lower arc rotation current shows positive effect on weld tensile strength as it reduces the width of LB zone at the weld interface. Similarly lower arc rotation current and shorter arc rotation time show positive effect on weld tensile strength as narrow LB zone results at the weld interface.

3.4 Bend Test

Bend test has been carried out for MIAB welded carbon steel tubes to assess the weld ductility (Table 3). Most of the samples show no open discontinuity with good weld ductility (Fig. 13). All the samples welded with higher upset current show no open discontinuity. On the other

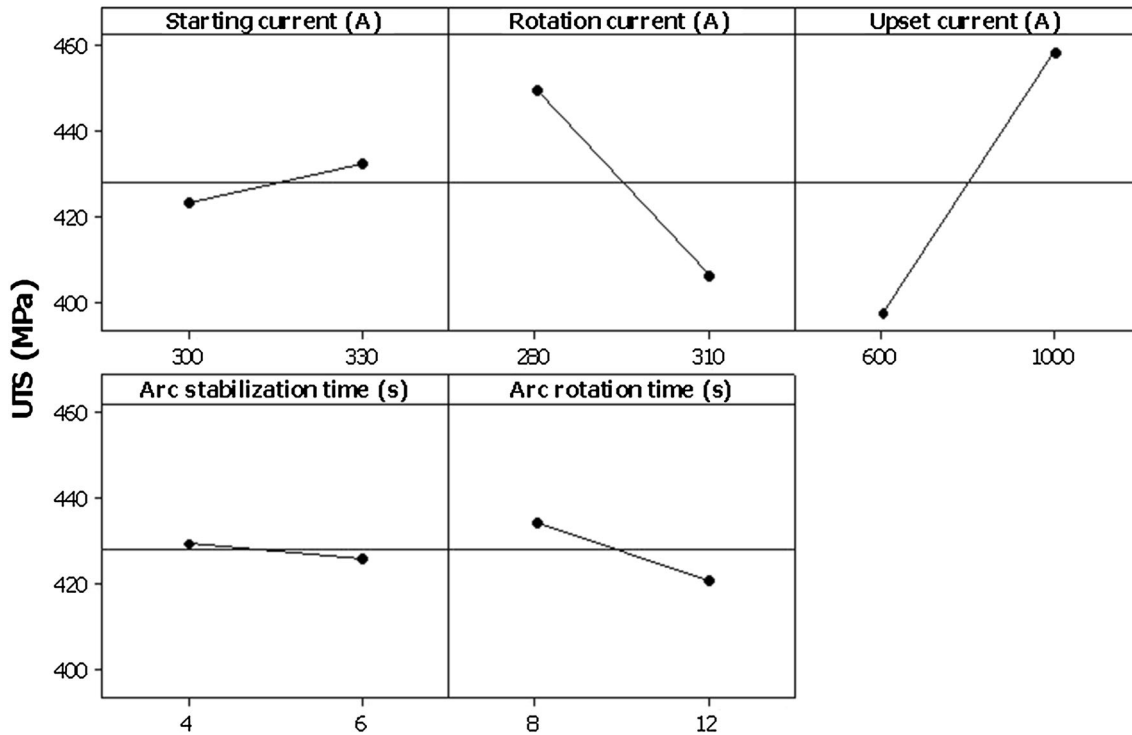
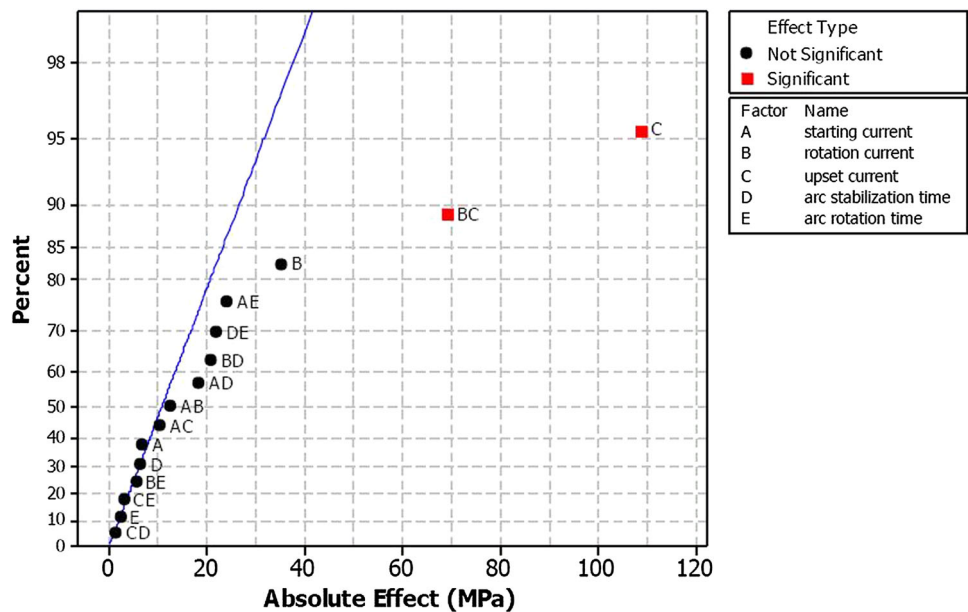


Fig. 10 Individual effect plots of weld variables on weld UTS

Fig. 11 Half normal effect plot for weld UTS response ($\alpha = 0.05$)



hand, the samples (CS/2, CS/12, CS/13 and CS/14) welded with lower upset current, show cracking during bend test. Bend test specimens usually exhibit cracks when it has brittle structure. But as discussed earlier, samples welded with lower upset current have LB zone containing softer microstructure. Hence in MIAB weld specimens, the cracking is not due to the presence of brittle phase in the weld structure. Instead, the impurities due to incomplete

expulsion lead to cracking. Due to lower upset current, the oxide impurities are retained in the weld interface without being expelled as flash.

In contrast to tension test results, the samples welded with lower arc rotation current and lower upset current fail more frequently compared to samples welded with higher arc rotation current and lower upset current. Apart from melting, arc rotation current also plays a significant role in

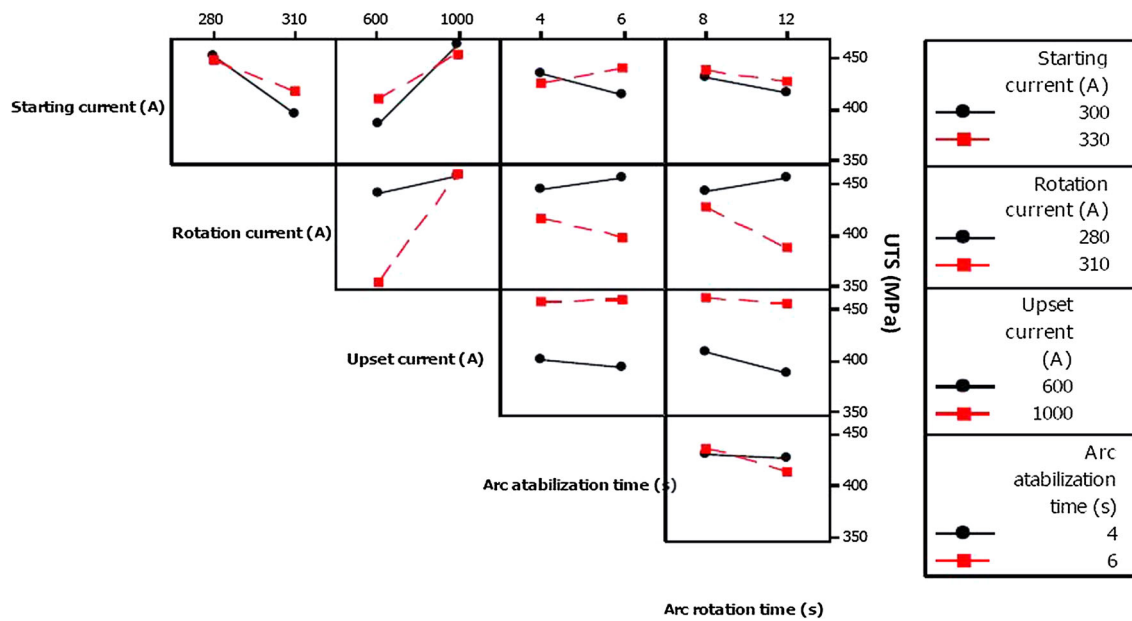


Fig. 12 Interaction effect plots of weld variables on weld UTS

Table 3 Bend test results for MIAB welded carbon steel tubes

Sample I.D	Root bend test	Face bend test
CS/1	No open discontinuity	No open discontinuity
CS/2	Open discontinuity	No open discontinuity
CS/3	No open discontinuity	No open discontinuity
CS/4	No open discontinuity	No open discontinuity
CS/5	No open discontinuity	No open discontinuity
CS/6	No open discontinuity	No open discontinuity
CS/7	No open discontinuity	No open discontinuity
CS/8	No open discontinuity	No open discontinuity
CS/9	No open discontinuity	No open discontinuity
CS/10	No open discontinuity	No open discontinuity
CS/11	No open discontinuity	No open discontinuity
CS/12	Open discontinuity	No open discontinuity
CS/13	Open discontinuity	Open discontinuity
CS/14	No open discontinuity	Open discontinuity
CS/15	No open discontinuity	No open discontinuity
CS/16	No open discontinuity	No open discontinuity

removing impurities from weld interface. In MIAB welding, the magnitude of the arc rotation current decides the arc acceleration during welding [3]. With higher arc rotation current, the arc acceleration increases and impurities are brought towards the outer diameter of the tube [21]. Upon upsetting, these impurities are removed as flash but with lower arc rotation current, the arc acceleration is less and impurities are not brought to outer diameter of the tube. With lower upset current, retention of impurities take place due to incomplete expulsion. Thus the lower arc



Fig. 13 Bend test specimen

rotation current and the lower upset current cause lower ductility with retained oxide impurities at the weld interface.

3.5 Conclusions

- Welded tubes show a distinct white zone i.e. Light Band (LB) zone at the weld interface in the samples welded using lower upset current. This is due to the incomplete homogenization and incomplete expulsion of decarburized region at the weld interface.
- Microstructural analysis shows three distinct TMAZs between the weld interface and unaffected base metal. At TMAZ I, welding parameters show a significant effect on microstructural transformations.

- In samples welded using lower upset current, TMAZ I shows LB zone containing fully ferritic structure at weld interface. Microstructural analysis confirms that the decarburization at weld interface is due to incomplete expulsion with lower upset current.
- Samples welded using higher upset current even with large variation of other welding parameters, exhibit high weld strength and ductility due to the formation of acicular ferrite.
- Sample welded with lower upset current have low strength and ductility due to formation of LB zone of sizable width, which is the result of decarburization and retention of impurities upon incomplete expulsion.

References

1. Yapp D, and Blackman S A, *J Braz Soc Mech Sci* **1** (2004) 89.
2. Taneko A, Arakida F, and Takagi K (Nippon Kokan Koji K.K), *J Jpn Weld Soc* **4** (1986) 570.
3. Kim J W, and Choi D, *P I Mech Eng B-J Eng* **217** (2003) 1401.
4. Vendan S A, Manoharan S, Buvanashakaran G, and Nagamani C, *Int J Adv Manuf Technol* **43** (2009) 1144.
5. Iordachescu D, Iordachesc M, Georgescu B, Miranda RM, Ruiz-Hervias J, and Ocana J L, *J Mater Process Technol* **210** (2010) 951.
6. Vendan S A, Mundla S R, and Buvanashakaran G, *Mater Manuf Process* **27** (2012) 573.
7. Sivasankari R, Balusamy V, Buvanashakaran G, Venkateswaran P R, and Kumar K G, *Def Technol* **11** (2015), 244.
8. Zak J and Rys P, *Weld J* (1972) 272.
9. Oshkaderov S P, *Phys Met Metallogr+* **110** (2010) 557.
10. Babu SS, *Curr Opin Solid State Mater Sci* **8** (2004) 267.
11. Prokic-cvetkovic R, Milosavljevic A, Popovic O, and Kovacevic K, *Struct Integr Life* **5** (2005) 31.
12. Yang J R, Huang C Y, and Huang C F, *J Mater Sci* **30** (1995) 5036.
13. Díaz-Fuentes M, Iza-Mendia A, and Gutiérrez I, *Metall Mater Trans A*, **34A** (2003) 2505.
14. Lee CH, Bhadeshia H K D H, and Lee HC, *Mat Sci Eng A-Struct* **360** (2003) 249.
15. Yang J R, Huang C Y, and Chiou C S, *ISIJ Int* **35** (1995) 1013.
16. Rasouli D, Asl. S K, Akbarzadeh A, and Daneshi G H, *J Mater Process Technol* **206** (2008) 92.
17. Smirnov M A, Pyshmintsev I Y and Boryakova A N, *Metallurgist+* **54** (2010) 444.
18. Todorov R P, and Khristov K G, *Met Sci Heat Treat+* **46** (2004) 1.
19. Wang JP, Yang ZG, Bai BZ, and Fang HS, *Mat Sci Eng A-Struct*, **369** (2004) 112.
20. Eghbali B, and Abdollah-zadeh A, *J Mater Process Technol* **180** (2006) 44.
21. Sato T, Katayama J, Ioka S, and Otani M, *Weld Int* **5** (1991) 5.